Mat. Res. Soc. Symp. Proc. Vol. 668 © 2001 Materials Research Society

Voltage Dependent Carrier Collection in CdTe Solar Cells

D.L. Bätzner[1], Guido Agostinelli[2], A. Romeo[1], H. Zogg[1] and A.N. Tiwari[1]
[1]Thin Films Physics Group, Laboratory for Solid State Physics,
Swiss Federal Institute of Technology Zurich,
Technopark, ETH-Building, Technoparkstr.1, CH-8005 Zurich
Tel: +41-1-4451472, Fax: +41-1-4451499; E-mail: baetzner@phys.ethz.ch
[2]European Commission, Joint Research Centre, 21020 Ispra (VA), ITALY

ABSTRACT

The measurement of quantum efficiency with bias voltage is a powerful tool to characterize CdTe/CdS solar cell. As the quantum efficiency changes drastically with bias it will be referred to as Apparent Quantum Efficiency AQE. The AQE gives insight to the spectral contents of the cell current and therefore resolves the spatial carrier collection in the cell at each working point. So it is possible to understand the influence of the junctions and changing resistances in the cell. The photoconductivity of CdS facilitates AQE well above unity, i.e. up to 100, at high forward bias. The spectral sensitivity of the CdS photoconductivity affects the cell current strongly. This can explain the dependence of fill factor and roll-over of the I-V characteristics on the spectral content of illumination. Further more back contact junction influence and defect related features, such as sub band gap generation, are evident in the AQE for high forward bias.

INTRODUCTION

The quantum efficiency QE of a solar cell gives valuable information about the spectral composition of the cells current, which is determined by the carrier generation and collection profiles $g(x,\lambda)$ and $f(x)$ respectively. The QE is defined at short circuit conditions with bias illumination to keep the cell at a reasonable injection level. QEs measured with applied bias voltage and different injection levels can vary significantly from the defined QE and therefore are referred to as apparent quantum efficiencies AQEs. The AQE(V) is determined by the magnitude of shunt and series resistance, junctions and their space-charge layers widths and blocking (presence of reverse diodes, e.g. back contact) effects. It can be expressed as the sum of two major contributions. The bulk collection and collection connected to a 'gain medium'.

VOLTAGE DEPENDENT QUANTUM EFFICIENCY MEASUREMENTS

The quantum efficiencies have been measured with lock-in-technique in the range of 300 nm to 1050 nm using a grid-monochromator. Signal and phase have been monitored with an EG&G lock-in-amplifier. A custom made trans-impedance-amplifier was used to apply bias voltage in order to keep the cell at the adjusted work point during measurements. The AQEs were measured without and with bias illumination of around 200W/m^2 to prevent the heating of the cell. I-V measurements under Standard Test Conditions and in the dark completed the characterization of the cells as well as C-V measurements in the dark.

From the C-V characteristics the depletion layer width as function of bias voltage $W_{pn}(V)$ for the pn-junction and the back contact junction $W_{bc}(V)$ have been calculated. Estimations for the effective minority carrier diffusion length L_{eff} in the bulk were made from C-V characteristics.

The voltage dependent apparent quantum efficiency AQE(V) measurements can be divided in three main regions. Region I from about 300 nm to 600 nm, region II from about 600 nm to 800 nm and region III from about 800 nm to 1000nm, i.e. the band edge region of CdTe. Region I is further divided in a 'blue' part between 300 nm and the absorption edge of CdS (~515 nm) assigned here as region Ia and region Ib from about 515 nm to 600 nm. Region III is as well subdivided in region IIIa from about 800 nm to the band gap of CdTe (~850 nm) and region IIIb – the sub band gap region – from about 860 nm to 1000 nm. These regions are illustrated in figure 1 together with the typical AQE(V) characteristics for CdTe/CdS solar cells.

All AQE(V) measurements for different cells show the same systematic behavior. For reverse bias the AQE increases in the region II and towards the absorption edge of CdTe. In forward bias the AQE decreases in region II, region Ib and region III. At a threshold, depending on the CdS layer thickness around 0.5 V - 1 V, the AQE in region Ia increases to values much higher than 1. At the same time the AQE in region Ib also starts to increase. For even higher bias an increase of AQE in region IIIa is occurring. Figure II gives a more detailed understanding of the different region plotting the AQE for a single wavelength of each region vs. the applied bias.

AQE FOR THE DIFFERENT WAVELENGTH REGIONS

Region II

Resistive effects and variation of the depletion layer width dominate the AQE(V) of region II. The series resistance is the main responsible for reduced QE at forward biases. Figure 2 illustrates the resistive effect depending on bias. The AQE is principally given by the absolute of the current difference in light and dark which decreases towards higher bias and converges against zero. A quantitative description of the phenomenon is given in [2]. The bias dependency of the depletion layer width W_{pn} also plays a role. At reverse bias, W_{pn} is extended and therefore more carriers get collected, assuming L_{eff} is not affected by bias. In forward direction the AQE decreases because W_{pn} shrinks and less carriers diffuse to the separating pn-junction. [3] gives calculations for this case. The spectrum towards longer wavelengths should be affected stronger,

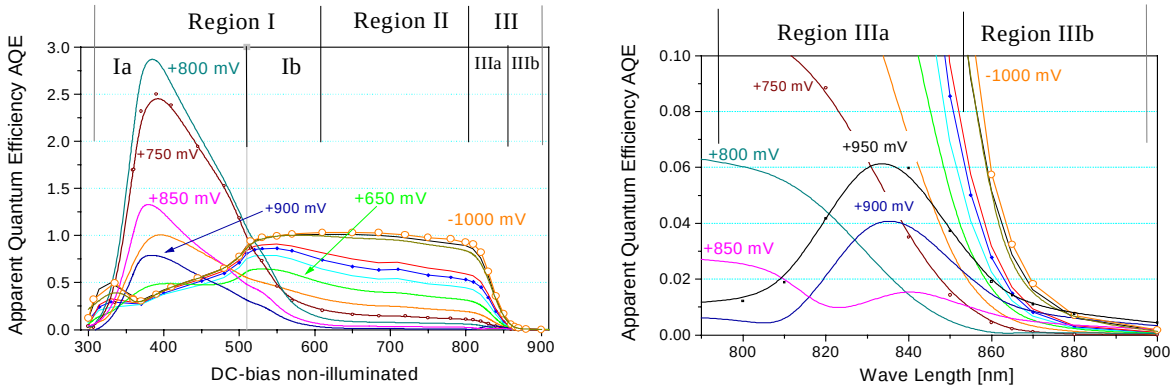

Figure 1. Apparent quantum efficiencies at various bias (dark). The AQEs are classifiable in 3 principal regions.

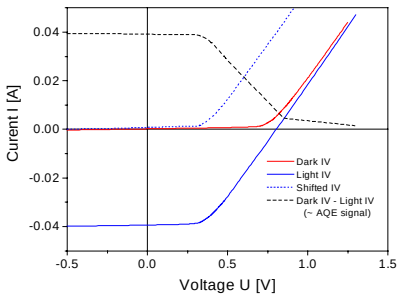

Figure 2. Schematic I-V characteristics in dark and light and upward shifted light I-V characteristics. The according AQE is given by the current difference in dark and light

as the penetration into the CdTe bulk is deeper. The limit for AQE in region II is unity for cells without cross-over and could exceed it for cross-over cells.

Region III

The AQE of region IIIa is affected like described for region II. In case of CdTe/CdS solar cells usually a cross-over in the I-V characteristics is observed. The consequence is that |AQE| drops to 0 towards the cross-over bias V_{cr} (which depends on λ as well) and starts to rise again for bias higher than V_{cr}.

Additionally a junction at the back contact contributes to the |AQE|. For high forward bias the back contact diode is in reverse direction and hence the depletion layer width W_{BC} starts to increase. The deep penetrating long wavelength irradiation generates carriers within a diffusion length from the (increased) Schottky diode space charge region. Those collected and yield a current towards the back contact, which is reverse to the junction current as indicated by a 180° phase shift in the AQE signal.

The same phenomenon is seen below the CdTe band gap (<1.44 eV) in region IIIb. The 180° phase shift is even more abrupt. This can only be explained by sub band gap carrier generation, e.g. from shallow traps. In CdTe usually those are assigned to Cd-vacancy-complexes [1]. At the back contact the density of these Cd vacancy-complexes should be higher due to pre-contacting etching procedures, which remove Cd from the back surface, and the deposition of contacting semimetals and metals [4].

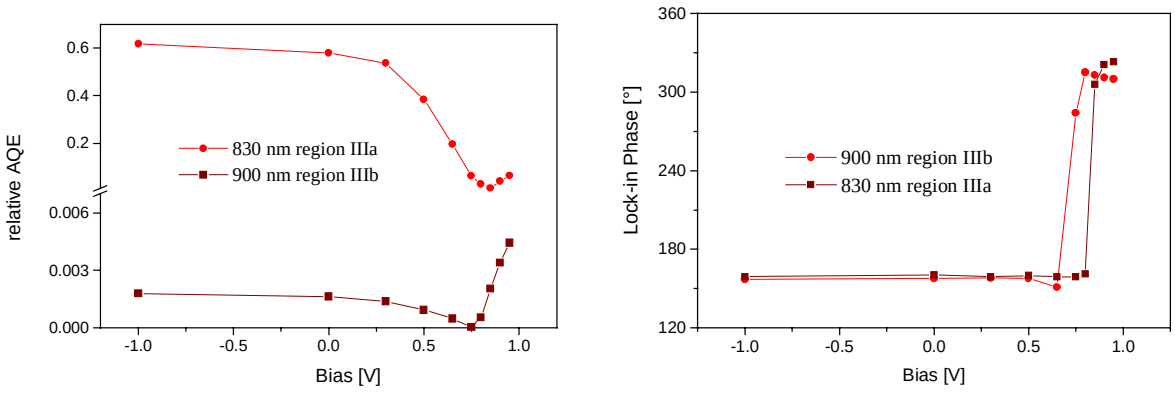

Figure 3. AQE (left) and phase (right) vs. bias for two wavelengths representing region IIIa and IIIb.

Region I

The AQE of region Ia measured in the dark seems unaffected by bias up to an intermediate threshold bias V_I. For the measured cells V_I was in the range of 0.3 V – 0.75 V and depended strongly on the CdS thickness which determines the effective resistance and the according voltage drop. Above the threshold bias V_I the AQE in region I starts to increase with bias of AQE values up to 100 (compare figure 4).

The most consistent explanation for such increasing quantum efficiencies far above unity for short wave lengths is the photoconductivity gain in CdS. The as deposited CdS is usually intrinsic and has a poor conductivity in the dark. With the carrier generation in CdS, defects get saturated [5] and the conductivity increases significantly, or the i-CdS barrier would be effectively lower, which is equivalent [6]. The applied bias forces a current through the cell, which can be many times higher than the maximum possible photon-generated current. The photoconductive gain is determined by the ratio of carrier transit time (through CdS) to the lifetime of the generated carrier [6]. With the applied bias the carrier transit time can be decreased but there is a maximum of achievable gain due to space-charge-limited current injection from the electrical contacts. For CdTe/CdS solar cells with strong roll-over the maximum gain and hence the maximum AQE is determined by the reverse diode saturation current. Photoconductive gain above unity occurs either by a voltage drop across a layer or the presence of a pnp-like structure. Since pn- or pin-junctions have a gain limit of 1, it can be inferred that the band diagram at the front contact of the device is more complicated and possibly yield a barrier.

The increase in AQE at forward bias above V_I is also apparent in region Ib (see figure 4), which is below the absorption edge of intrinsic CdS. This indicates either that there is also extrinsic photoexitation from sub band gap states or the presence of an intermixed CdS/CdTe layer with a band gap gradient and most likely a band gap quench. Further more the density of interface traps should be fairly high and support the extrinsic absorption, which would allow a certain photoconductive gain in region Ib as well.

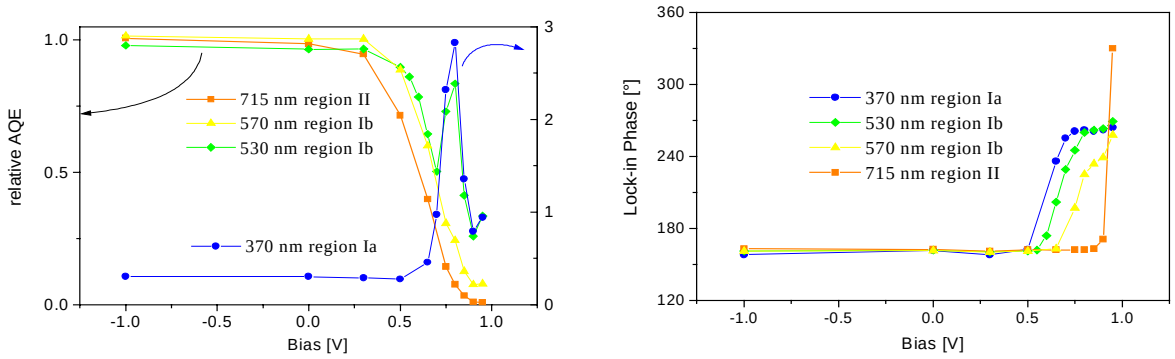

Figure 4: Absolute AQE (left) and phase (right) vs. bias for wavelengths of region Ia, Ib and II.

SIMULATION OF IQE

We developed a new yet still basic model to calculate the IQE. It already describes the qualitative behavior of the measured AQE in region II and III by assuming generation in 2 junctions, one at the front (pn-junction) and one at the back (postulated Schottky barrier). The

fact that these junctions are of opposite direction is considered by a negative current collected at the back contact. The inner quantum efficiency IQE is calculated with the generation profile g(x,λ) and collection function f(x) of the carriers.

$$IQE = \int g(x,\lambda) \bullet f(x)\, dx \qquad (1)$$

g(x,λ) is a function of the absorption coefficient α(λ) and the exponential decay of photon density in the bulk and the collection function is unity in the depletion layer and drops exponentially with L_{eff} like sketched in figure 5. The total |IQE| will be the difference of the $|IQE_{pn}|$ and $|IQE_{BC}|$. Additionally the sum of the collection functions $f_{pn}(x)$ and $f_{BC}(x)$ must not exceed unity. Geometry and simulation results at forward bias are shown in figure 5. Parameters for $W_{pn}(V)$, $W_{BC}(V)$ and L_{eff} (~1µm) were determined with C-V measurements. The current generation in the back contact space charge region increases with $W_{BC}(V)$.

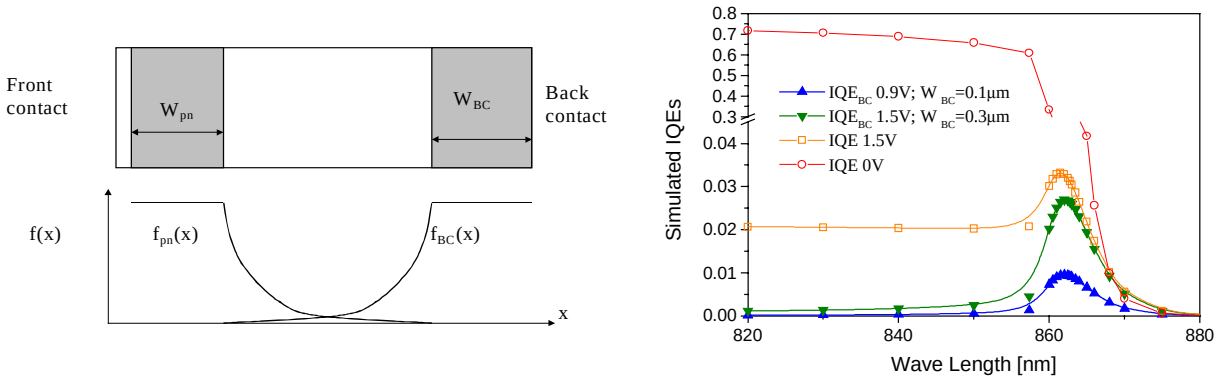

Figure 5. Geometry for simulation (left) and simulated IQEs at different bias (right; note the axis break). Solid symbols are for IQE contribution of the back diode; open symbols represent total IQE.

DISCUSSION

It is obvious that the thickness of the CdS determines the transmission of wavelengths below the absorption edge of CdS λ_{CdS} ~ 515 nm. For thin CdS (~200 nm) the blue part of the QE is high whereas the thick CdS (≥ 800 nm) shows almost no 'blue' response. Therefore the current

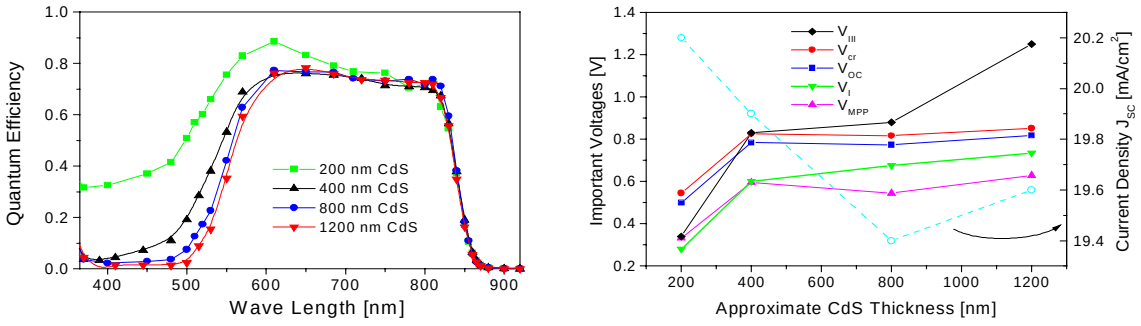

Figure 6. QE (left) and voltage parameters (right) vs. CdS thickness. Thin CdS has more blue response but much lower threshold voltages, especially open circuit voltage V_{OC}.

densities J_{SC} are little lower (~5%) but all voltage are significantly higher (~50%) as can be seen in figure 6. This suggests that the best pn-junction for photovoltaic performance is formed, using a rather thick CdS layer (for the applied PVD-process). Yet the blue light is not directly contributing to the current, it seems that it is crucial for the cell performance due to its effect on the conductivity of the CdS. As the cell with thick CdS has the highest V_{OC} the junction formation is best and the interface defect state density might be lowest.
As a rule of thumb for the threshold voltages of the AQE regions can be sorted with the cell parameters as follows: $V_{MPP} < V_I < V_{OC} < V_{cr} < V_{III}$. This does not completely apply to the cell with a thin CdS layer probably due to partial shunting and worse junction formation due to surface roughness of the CdS layer and post deposition activation treatment with $CdCl_2$.

CONCLUSION

Voltage dependent carrier collection was studied with quantum efficiency measurement at different bias. The measured AQE of CdTe/CdS solar cells have been classified in 3 regions. Region I is dominated by the photoconductive gain in CdS at forward bias beyond V_{MPP} due to blue light absorption. Region II follows the voltage dependency of a classic solar cell, i.e. resistance and junction width effects. Region III becomes dominated by the collection in the back contact barrier for bias beyond V_{OC}. Region Ib and IIIb for energies lower than the band gap of CdS or CdTe respectively indicate the sub band gap generation and presence of shallow traps.

We assume the AQE » 1 can only be achieved with the photoconductive gain of a pnp-like device structure (or a strong voltage drop across the CdS layer). The consequence is a barrier that is probably located in the front of the cell and could rise from and intrinsic layer of CdS.

A basic model to simulate quantum efficiencies could qualitatively demonstrate the influence of the back contact junction on AQE. A more refined model for a quantitative analysis of the AQEs with the cell parameters L_{eff}, W_{BC}, W_{pn} and parameters for cell resistance and CdS photoconductivity is in development.

ACKNOLEDGEMENTS

We gratefully acknowledge Stefan Brachmann from Fraunhofer ISE for measurement equipment design and support.

REFERENCES

[1] T. L. Chu, Current Topics in Photovoltaics **3**, 242 (1988)
[2] J. Sites, H. Tavakolian, R.A. Sasala, Solar Cells **29,** 39-48 (1990)
[3] X. X. Liu and J. Sites, Journal of Applied Physics **75**(1), 577 (1994) 577
[4] D. L. Bätzner, A. Romeo, H. Zogg, A. Tiwari, R. Wendt, Thin Solid Films **361-362**, (1-2) 463-467 (2000)
[5] I. L. Eisgruber, J.E. Granata, J.R. Sites, J. Hou, J. Kessler, Solar Energy Materials and Solar Cells **53**, 367-377 (1998)
[6] R. H. Bube, *Photoelectronic Properties of Semiconductors*, (Cambridge Press, 1992) Cap. 2